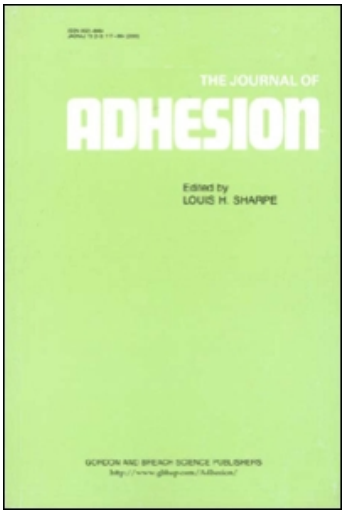

The Journal of Adhesion

Publication details, including instructions for authors and subscription information:
http://www.informaworld.com/smpp/title~content=t713453635

Surface Forces and the Adhesive Contact of Axisymmetric Elastic Bodies

A. -S. Huguet[a]; E. Barthel[a]

[a] Laboratoire CNRS/Saint-Gobain "Surface du Verre et Interfaces", 39, quai Lucien Lefranc, Aubervilliers Cedex, France

To cite this Article Huguet, A. -S. and Barthel, E.(2000) 'Surface Forces and the Adhesive Contact of Axisymmetric Elastic Bodies', The Journal of Adhesion, 74: 1, 143 — 175

To link to this Article: DOI: 10.1080/00218460008034528

URL: http://dx.doi.org/10.1080/00218460008034528

J. Adhesion, 2000, Vol. 74, pp. 143–175
Reprints available directly from the publisher
Photocopying permitted by license only

Surface Forces and the Adhesive Contact of Axisymmetric Elastic Bodies

A.-S. HUGUET and E. BARTHEL*

Laboratoire CNRS/Saint-Gobain "Surface du Verre et Interfaces", 39, quai Lucien Lefranc, BP 135, F-93303 Aubervilliers Cedex, France

(Received 3 June 1999; In final form 4 October 1999)

A synthetic approach to the problem of the adhesive contact of axisymmetric elastic bodies is proposed. A convenient and general formulation is thus obtained, which is shown to yield directly most of the useful models. In particular, the roles of the shape of the indenter on the one hand, and of the nature of the attractive interactions on the other hand are clearly separated. By nature, this approach can also be used in the case where the bodies are in interaction but not in contact. This results in a consistent treatment of long-range interactions and contact properties.

Keywords: Contact mechanics; Adhesion; Surface forces

1. INTRODUCTION

The problem of the adhesive contact of elastic bodies is basically well understood. Historically, the first attempt, by Derjaguin, in his otherwise famous paper on the Derjaguin approximation [1], was quite disappointing: he found a pull-off force equal to πwR, where w is the adhesion energy and R the radius of the sphere. However, this result was at variance ("Daher ergibt sich ein zweimal so kleiner Wert [...]" [1]) with the just-discovered Derjaguin approximation, which describes the non-contact part of the same force curve and predicts a force

*Corresponding author. Tel.: 33148 395557. Fax: 33148 347416. e-mail: etienne.barthel@sgr.saint-gobain.com

twice as large at zero distance. This was the first attempt at matching long-range forces and pull-off force. Later, Derjaguin apparently reconciled his theories, since the DMT model [2] does predict a pull-off force equal to $2\pi wR$. As a result, continuity between the contact and non-contact parts of the force curve was restored (Fig. 1). There remained a question, however: the slope of the DMT curve at zero distance is zero, while a typical non-contact force curve is expected to exhibit a non-zero derivative at zero distance. Consequently, there apparently still is a discontinuity in the *derivative* of the force curve, a somewhat puzzling result. In addition, in the meantime, Johnson, Kendall and Roberts had put forward a model [3] giving a pull-off force equal to $3\pi wR/2$. The ensuing controversy was solved when, following Tabor [4], numerical computations [5–8] showed that the two models could be considered as limits in a continuous transition. The relevant parameter was shown to be the ratio of the gap between the surfaces just outside the contact zone and the range of the interactions (this ratio is denoted [5, 9] μ or λ). The JKR model applies when λ is much larger than unity. In this case, clearly, the non-contact part of the force curve is almost non-existent. The DMT model, on the contrary, applies when the range of the interactions is large ($\lambda \ll 1$), and matching the two parts of the force curve remains an open issue.

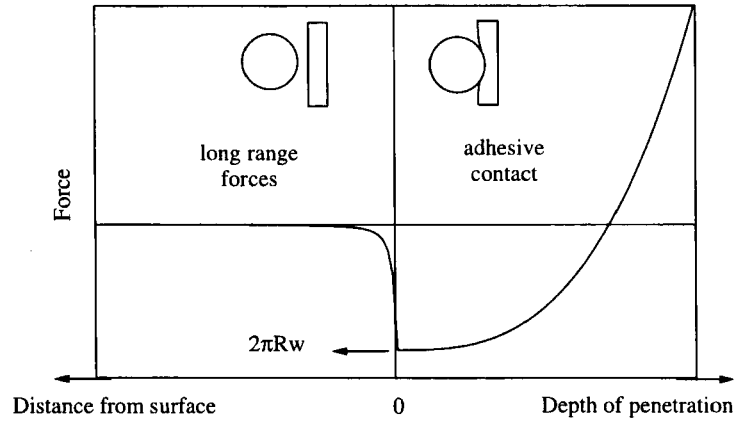

FIGURE 1 Typical matching problem for the non-contact (long-range forces) part of a force curve described by the Derjaguin approximation and the contact part of the same force curve described by the DMT model: although the force curve is continuous at zero distance (equal to $2\pi Rw$), the derivative is not (*cf.* also Fig. 6).

Simultaneously, the JKR model was studied through a rather different approach, in terms of fracture mechanics [10–12]. The culminating point of the fracture mechanics approach was reached in 1992, when Maugis proposed a Dugdale model for the adhesion of spheres [9]. This paper brought a number of fruitful ideas, allowed the first analytical description of the transition, and trigerred a number of additional contributions along this line [13–17].

Following these recent advances, we try to provide a compact general formulation of the adhesive contact of axisymmetric elastic bodies and also to describe the non-contact part of the experimental curves within the same theory.

Thus, we first give general expressions for the force and penetration assuming a given attractive stress distribution outside the contact zone and a given shape of the indenter. As a result of the adhesive process, two phenomena are simultaneously observed: compared with the non-adhesive case (Hertz [18]),

1. the contact zone increases (as in the JKR model);
2. there is an additional tensile force (as in the DMT model).

We discuss their relative weight in the general solution in terms of lateral extension of the attractive *interaction zone c* (Fig. 2). In this

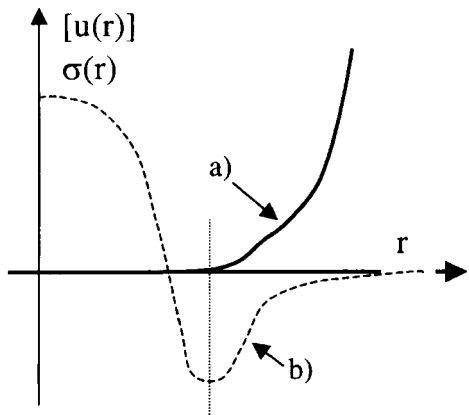

FIGURE 2 Typical gap profile (full line) and stress distribution (dashed) of an indenter in adhesive contact with a flat non-deformable surface. The radius of the contact zone is *a*, the radial extension of the interaction zone is *c*.

manner, the mechanics of the adhesive contact problem, and in particular of the JKR and DMT limits, can be obtained. Up to that point the description can be applied to an arbitrary type (in terms of range or reversibility, for example) of attractive interaction.

Then, we will assume a more specific description of the adhesive process in terms of interaction *potential* and, thus, of *adhesion energy*. Using the previous expressions for the mechanical response of the surface, we show in the general case that, when the interaction is short-ranged, the contact-zone-increase effect accounts for the full adhesion energy and, thus, obtain the generalization of the JKR model to bodies of arbitrary shapes. We also show that the linear elastic fracture mechanics approach (in terms of energy release rate) is easily derived from the previous expressions. In the case of long-range interactions, we show that the DMT limit is obtained only for paraboloidal bodies (which is the usual approximation for the sphere). The same limit is either basically useless or does not exist for other shapes. For intermediate cases, we propose a rationalization of the approximation schemes developed so far.

Finally, we outline the treatment of the non-contact part of the force curve and give an example of the consistent treatment of long-range and contact parts of an experimental force curve. This example is illustrative of the improvement obtained by the proposed modeling.

2. DESCRIPTION OF THE PROBLEM

2.1. Self-consistency

The adhesive contact between two bodies is a process which involves two phenomena:

1. the interaction between the bodies, through surface forces,
2. the mechanical deformation of the bodies.

The complexity of the problem comes from the fact that these phenomena are interdependent: the mechanical deformation will obviously depend upon the interaction and the interaction will depend upon the distance between the surfaces and, hence, upon the deformation of the bodies. It follows that a self-consistent solution is required.

Note, however, that these two phenomena are also at work when the surfaces interact without contact. In this case, however, one will usually consider that the surfaces are non-deformable – because mechanical instability of the experimental device will usually occur before the deformations are sizable – and the Derjaguin approximation [1] will be used. That this is not necessarily correct will be shown below.

2.2. Contact Zone and Interaction

The initial question one is faced with, for a given problem, is thus to describe both the mechanical behavior of the solids and their interaction. However, in doing so, one should keep in mind that the division of the phenomena between surface interaction and mechanical behaviour may in some cases be quite artificial.

More specifically, it is clear that the interaction potential between surfaces is always repulsive at small distance. This is due to Born repulsion between atoms, and ensures the stability of matter. Now, it is not trivial to get an accurate description of this repulsion. An *ad hoc* potential like the d^{-12} used in the Lennard-Jones potential is simply indicative of the trend. Actually, an approximation scheme can be devised, which retains the main feature of this repulsive part of the potential: its very steep variation with distance. Thus, a very small change in distance will induce a very large change in interaction. Or, conversely, the interaction can take on an arbitrary value – within the bounds of allowed values (maximum tensile stress and elastic limit) – with almost no change in separation. As a result, the problem can be reformulated in the following way: there is a zone in which the distance is prescribed and the stress is free. This is, of course, the contact zone. Thus, we have turned a prescription on the interaction into a prescription on the mechanics: the displacement is fixed in the contact zone.

As a result, there are, broadly speaking, two families of approaches:

1. one can prescribe the full interaction (attractive and repulsive parts) and, from the knowledge of the surface response to externally-applied stress, try and solve the self-consistent problem [5, 7, 8, 19]

or

2. one can exclude the very short range repulsive part of the interaction and work out the solution using mixed boundary conditions

for the mechanical side of the problem: the displacement is prescribed inside the contact zone and the stress outside [2, 3, 9, 16, 18, 20].

The interactions outside of the contact zone may be very diverse. The many types of interactions known in the field of surface forces may be operating – chemical interaction, electrostatic, electrical double-layer, meniscus force, ... – including the van der Waals force, which, although a body force, turns into a surface force when volume integration is performed on bodies with small curvature [21]. In addition, non-conservative forces, like viscous dissipation at the periphery of the contact zone, may also be considered [10]. In fact, the approach we present is independent of the nature of the interaction as long as it is a surface interaction, *i.e.*, it results in a surface stress distribution.

Once these questions have been sorted out, we cannot proceed until the description of the mechanical behaviour of the surface under given boundary conditions is known.

3. SURFACE ELASTICITY: USEFUL RESULTS

This technical section deals with the response of an elastic flat surface: the aim is to formulate general expressions for the total force, displacement and elastic energy in terms of an auxiliary function, g. We also show how g depends upon the surface stress distribution, or upon the normal surface displacement.

The present formulation relies upon results for the description of the elastic response of a flat surface known in the literature [22–29]. We have tried, in the Appendices, to provide a complete and "minimal" (in term of complexity) derivation of those results which are necessary here by consistently using the Fourier transform method (as suggested by Landau [30], page 26, note 1). Although it differs in a number of details, this approach is, thus, essentially Sneddon's [22]. We believe, however, that the present derivation side-steps several more difficult points in Sneddon's texts. In addition, it directly provides some necessary relations (Eqs. (3.10) and (3.11)) usually not reported in the literature.

3.1. Surface Displacement

Let us assume linear elastic behaviour, a frictionless contact and an axisymmetrical geometry. In particular, we are interested in the surface displacement, $u_z(r)$, induced by a normal stress distribution at the surface, $F_z(r)$.

We will be using the result that:

$$u_z(r) = \frac{2}{\pi}\frac{1}{\mathcal{K}}\int_0^r \frac{g(t)}{(r^2 - t^2)^{1/2}}\,dt, \tag{3.1}$$

where the g function thus introduced is

$$g(t) = \int_t^{+\infty} \frac{sF_z(s)}{(s^2 - t^2)^{1/2}}\,ds, \tag{3.2}$$

and

$$\mathcal{K} = \frac{E}{2(1 - \nu^2)}. \tag{3.3}$$

Note the factor 3/8 with the frequent definition

$$K = \frac{4E}{3(1 - \nu^2)} \tag{3.4}$$

which is linked to the case of the spherical indenter, and the factor 1/2 with the usual definition

$$E^* = \frac{E}{1 - \nu^2}. \tag{3.5}$$

The important fact here is that according to Eq. (3.1), the surface displacement at r is obtained through the datum of the auxiliary function $g(s)$ for $s < r$ only. Conversely, $g(r)$ is known from the datum of $F_z(s)$ for $s > r$ only (Eq. (3.2)). This property will prove invaluable in the context of mixed boundary conditions which appears in the adhesive contact problem (Section 4).

3.2. Surface Stress

One of the main features of Eqs. (3.1) and (3.2) is that they can be inverted. In the present derivation (Appendices), which is based on the

successive use of Hankel and cosine transforms, this property stems from the fact that each of these transforms is invertible. Explicitly, one gets:

$$g(t) = \mathcal{K}\frac{\partial}{\partial t}\int_0^t dr \frac{r u_z(r)}{(t^2 - r^2)^{1/2}} \tag{3.6}$$

$$= \mathcal{K}\left[u_z(r=0) + t\int_0^t dr \frac{u_z'(r)}{(t^2 - r^2)^{1/2}}\right], \tag{3.7}$$

and

$$sF_z(s) = -\frac{2}{\pi}\frac{d}{ds}\int_s^{+\infty} dt \frac{tg(t)}{(t^2 - s^2)^{1/2}} \tag{3.8}$$

or

$$F_z(s) = \frac{2}{\pi}\left[\frac{\Delta g(s_0)\Theta(s_0 - s)}{(s_0^2 - s^2)^{1/2}} + \int_s^{+\infty} dt \frac{g'(t)}{(t^2 - s^2)^{1/2}}\right] \tag{3.9}$$

Equations (3.7) and (3.9) were obtained by integrating by parts. We also provided for the possibility that g be discontinuous by introducing the jump $\Delta g(s_0)$ of g at s_0. Equivalent relations were introduced by Sneddon under the denomination of Abel's relation [31].

Here again, Eqs. (3.6) or (3.7) express $g(t)$ from the datum of $u(r)$ for $t > r$ only, while the surface stress at s is obtained through the datum of the auxiliary function $g(t)$ for $s < t$ only (Eqs. (3.8) and (3.9)).

Note that this is just the general form of the results Maugis used in his paper [9]; although, since these equations do not exist as such in Sneddon's papers, he had to build them up, in a special case, by linear superposition of two particular cases [31, 32].

3.3. Force and Energy

Computing the total force, F, applied to one of the bodies through the interface as a function of the auxiliary function, g, we obtain

$$F = 4\int_0^{+\infty} ds\, g(s). \tag{3.10}$$

Similarly, the total mechanical energy, $\mathcal{E}$, is

$$\mathcal{E} = \frac{2}{K} \int_0^{+\infty} ds\, g^2(s). \tag{3.11}$$

Following our approach (Appendix B), these relations are again obtained through general properties of the Hankel and cosine transforms.

4. GENERAL EQUATIONS FOR THE AXISYMMETRICAL CONTACT

We now further investigate the properties of the g function. We show that, in the contact problem, g can be calculated from the boundary conditions – *i.e.*, the shape of the indenter and the nature of the interactions – from Eqs. (3.1) and (3.2) and their inverses. Further, we also show that, in addition to the total force and elastic energy (Section 3.3), the *penetration* of the indenter can also be expressed as a function of g, thus completing the general solution to the contact problem.

Let us consider an axisymmetrical deformable body with convex shape $h(r) > 0$ (with $h(0) = 0$) in contact with a perfectly rigid flat plane. We assume there is a contact zone of radius a. Outside the contact zone, we suppose there is a normal stress distribution, $p(r)$, which acts on the bodies. No specification as to the form and origin of this stress distribution is given. In particular, no reference to the adhesive mechanism is used for now.

The boundary conditions are, thus:

$$u_z(r) = \delta - h(r) \quad \text{when } r < a, \tag{4.1}$$

$$F_z(r) = -p(r) \quad \text{when } r > a. \tag{4.2}$$

Since the interaction outside the contact zone is assumed to be attractive, $p > 0$. Inward displacement, u_z, is counted positive. Similarly, the penetration, δ, will be counted positive if interpenetration would result, were the bodies non-deformable.

The solution to the adhesive contact problem then proceeds as follows: from the boundary condition (4.1) [resp., (4.2)] and Eq. (3.7) [resp., (3.2)], the g function can be calculated for $r < a$ [resp., $r > a$]. Matching these two parts of the function g for continuity (which results from the continuity of stress at a) gives an equation from which the penetration is obtained. Then, the total force is calculated through (3.10). Of course, all the other quantities in the problem can also be derived from g, such as the stress distribution inside the contact zone (Eq. (3.8)), the surface displacement outside the contact zone (Eq. (3.1)) and the total elastic energy (Eq. (3.11)).

4.1. A Singular Case: The Flat Punch

As a first example, we show how to calculate the solution for the adhesionless ($p(r)=0$ for $r > a$) rigid flat punch of radius a indenting the plane down to a penetration δ_{fp}, a well-known result due to Boussinesq [20]. We here have $h=0$. Let us determine the g function from the boundary conditions. We use Eqs. (3.7) and (3.2) from which we get:

$$g(t) = \mathcal{K}\delta_{fp} \quad \text{when } t < a, \tag{4.3}$$

$$g(t) = 0 \quad \text{when } t > a. \tag{4.4}$$

As a result, from Eq. (3.10), we obtain the relation between force and displacement

$$F_{fp} = 4\mathcal{K}a\delta_{fp}. \tag{4.5}$$

In addition, from Eqs. (3.1) and (3.9), we obtain the information complementary to the boundary conditions, *i.e.*, the displacement outside the contact zone and the stress distribution inside:

$$u_{z,fp}(r, z=0) = \frac{2}{\pi}\delta_{fp} \arcsin\left(\frac{a}{r}\right) \quad \text{for } r > a, \tag{4.6}$$

$$F_{z,fp}(r, z=0) = \frac{2}{\pi}\frac{\mathcal{K}\delta_{fp}}{(a^2 - r^2)^{1/2}} \quad \text{for } r < a. \tag{4.7}$$

4.2. General Solution for Non-singular Indenter Shapes

Let us now assume a regular shape for the indenter (*i.e.*, with a continuous derivative). Under the external loading and the adhesive interaction, the indenter penetrates the plane and the contact radius reaches a value a. We want to calculate expressions for the penetration, δ, and the force, F, as a function of a. Let us first calculate g. Denoting

$$\delta_0(t) = \frac{\partial}{\partial t}\int_0^t \frac{rh(r)dr}{(t^2 - r^2)^{1/2}} = t\int_0^t \frac{h'(r)dr}{(t^2 - r^2)^{1/2}}, \tag{4.8}$$

from Eqs. (3.7) and (3.2) we have

$$g(t) = K(\delta - \delta_0(t)) \quad \text{when } t < a, \tag{4.9}$$

$$g(t) = -\int_t^{+\infty} \frac{sp(s)ds}{(s^2 - t^2)^{1/2}} \quad \text{when } t > a. \tag{4.10}$$

4.2.1. Penetration

We now calculate the penetration, δ. If the shape of the indenting body, h, and its derivative, h', are continuous at a, then we have continuity of the normal stress at a and, thus, continuity of g, which allows us to determine δ in the following way.

Let us first consider the case of the non-adhesive contact. We know from Eq. (4.10) that $g(a) = 0$. Thus, the penetration is

$$\delta = \delta_0(a). \tag{4.11}$$

We conclude that the function $\delta_0(t)$, which only depends upon the shape of the indenter, is the penetration which is necessary to obtain a radius of contact, a, in the absence of attractive interaction [31]. The function δ_0 and all the subsequently-introduced functions are explicitly given for the case of the cone and the paraboloid in the Table.

TABLE Values of the various expressions describing the adhesionless contact for two different indenter shapes

	$h(t)$	$\delta_0(t)$	$\phi_0(t)$	$a\delta_0(a)-\phi_0(a)$	F_0
Cone	αt	$\pi/2\ \alpha t$	$\pi/4\ \alpha t^2$	$\pi/4\ \alpha a^2$	$\pi\mathcal{K}\alpha a^2$
Paraboloid	$t^2/2R$	t^2/R	$t^3/3R$	$2a^3/3R$	$8\mathcal{K}a^3/3R$

Similarly, in the case of the adhesive contact, the penetration, δ, is simply

$$\delta = \delta_0(a) + \frac{1}{\mathcal{K}} g(a). \tag{4.12}$$

Equation (4.12) means that attractive interactions reduce the penetration necessary to reach a contact radius, a, by a distance, $g(a)/\mathcal{K}$ (note that $g(a)$ is negative by definition). This increase of the contact zone due to the adhesive interaction – for which we obtain a general formulation – is the central concept in the JKR approach [3]. It clearly appears as a competition between the interaction, as weighted in $g(a)$, and the rigidity of the surface expressed by $\mathcal{K}$. We, thus, observe that some increase of the contact zone will be observed for any stress distribution, although $g(a)$ clearly emphasizes the contributions close to the contact zone.

4.2.2. Force

From Eqs. (3.10), (4.9) and (4.10), the total force is expressed as

$$F(a) = F_0(a) + 4ag(a) + 4\int_a^{+\infty} ds\, sp(s) \arcsin\frac{a}{s} - 2\pi\int_a^{+\infty} ds\, sp(s), \tag{4.13}$$

where F_0 is the force necessary for the adhesionless indenter to reach a contact radius a and reads

$$F_0(a) = 4\mathcal{K}\{a\delta_0(a) - \phi_0(a)\}, \tag{4.14}$$

with

$$\phi_0(t) = \int_0^t ds\, \delta_0(s). \tag{4.15}$$

We can picture this Hertz-like repulsive contribution as the force required to push a flat punch down to a penetration $\delta = \delta_0(a)$ minus a (positive) quantity which accounts for the reduction in resistance due to the upward sloping shape.

In order to describe the other contributions, which arise as a result of the attractive interaction, let us start from the adhesionless punch indenting the plane with a penetration δ (Fig. 3a). The radius of contact is a_{ini}, and the force is the bare Hertz contribution $F_0(a_{\text{ini}})$. If we switch an attractive interaction on, then an additional surface displacement occurs (Fig. 3b), Eq. (3.1), which increases the contact radius to a. However, this additional displacement has to be cancelled inside the contact zone, due to the boundary condition Eq. (4.1). Thus, the stress distribution inside the contact zone rearranges, so that the boundary conditions be fulfilled inside the contact zone while preserving the continuity of the stress distribution at a. Thus, the final stress distribution inside the contact but close to the contact line is tensile (Fig. 2).

As a result, the Hertz contribution increases to $F_0(a)$. In addition, a tensile stress distribution develops inside the contact zone, which is determined by the final radius of contact and the external stress

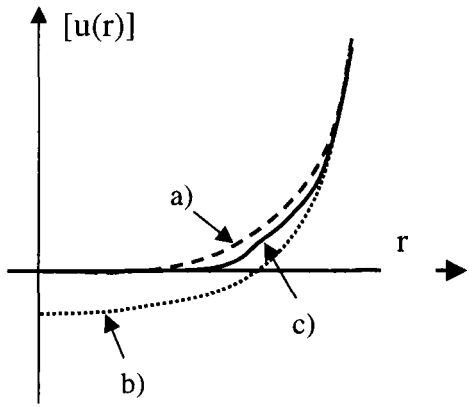

FIGURE 3 Gap profile of the indenter in contact with a flat non-deformable surface. (a) in the absence of attractive interaction; (b) with the additional displacement due to the attractive interactions alone; (c) with the additional displacement due to both the attractive interactions and the boundary conditions inside the contact zone.

distribution, and leads to the next two terms. Finally, the total force, F, breaks down into four components (Eq. (4.13)). The first term, $F_0(a)$, in Eq. (4.13) is the usual Hertz repulsive (*i.e.*, positive) component of the adhesionless punch with the final contact radius a. Thus, the increase in the contact zone has induced an increase in the repulsive Hertz term from $F_0(a_{ini})$ to $F_0(a)$. The second and third terms, F_{incr} and F_{add} form the contribution from the attractive stress distribution inside the contact zone. Note that F_{incr} (tensile) results from the global displacement, $g(a)/K$ (flat punch displacement), inside the contact zone, and reflects the contact zone increase effect. It is partially offset by F_{add} (compressive), which results from the cancellation of the surface displacement inside the contact zone due to the stress distribution outside. The last term, F_{ext} (negative), is the contribution from the stress distribution outside the contact zone.

We are also in a position to discuss the relative weight of the adhesive contributions in terms of the radial extension of the surface stress distribution and compare with the standard theories. If this extension is large compared with the radius of contact, examination of the various expressions shows that F_{ext} dominates and F_{incr} and F_{add} cancel at first order. Thus, the attractive stress is essentially *outside* the contact zone, does not bring about substantial increase of the contact zone but simply acts as an externally-applied force. This situation is reminiscent of the DMT model. On the contrary, if the range is small, F_{incr} dominates and the other two interaction terms cancel at first order. Thus, the contact zone increase effect is dominant, and the attractive stress is essentially *inside* the contact zone. In this case, the picture which emerges from Eqs. (4.12) and (4.13) is the additional flat-punch retraction (*cf.* Section 4.1 with a displacement $g(a)/K$) central to the JKR theory, and the contact is completely described by the specification of $g(a)$.

As an illustration, let us consider the case where the attractive stress is a constant inside the interaction zone, as assumed by Maugis [9]. We assume a radius of contact and an interaction amplitude equal to unity. Figure 4 displays the ratio of the absolute value of the various interaction force terms in this case as a function of the extension of the interaction zone, c.

Thus, we have given general expression for the two effects of attractive interactions:

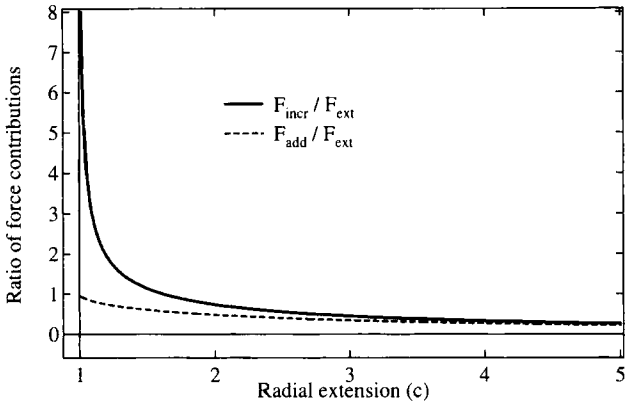

FIGURE 4 Absolute value of the relative magnitude of the three force contributions due to the attractive interaction as a function of the radial extension of the interaction zone, c, in the Maugis model [9]. The stress amplitude, σ_0, and the radius of contact a are chosen equal to unity. Note that F_{add} is positive, while F_{incr} and F_{ext} are negative. At small radial extension, F_{incr} dominates, while F_{add} and F_{ext} cancel (JKR limit). At large radial extension, F_{ext} dominate, while F_{incr} and F_{add} cancel (DMT limit).

1. by a wetting-like effect, they tend to increase the contact radius at a given penetration
2. they contribute an overall attractive force, F_{ext}.

The general behaviour results from the sum of these effects.

4.2.3. The Gap

Since the interaction between the contacting bodies will depend upon (at least) the local value of the gap, the self-consistent treatment of the problem requires the knowledge of the shape of the gap outside the contact zone. Thus, in this more technical subsection, we consider the deformations outside the contact zone in more detail.

Let us define the gap between the surfaces as

$$[u(r)] = u_z(r) - \delta + h(r). \tag{4.16}$$

Naturally, $[u(r)]$ is zero inside the contact zone. Outside the contact zone, the only non-trivial contribution comes from the deformation

$u_z(r)$, $r > a$. This deformation is the sum of the adhesionless term

$$u_{z,0}(r) = \frac{2}{\pi}\int_0^a \frac{\delta_0(a) - \delta_0(t)}{(r^2 - t^2)^{1/2}}\,dt, \tag{4.17}$$

and the term due to the adhesive interactions

$$u_{z,\mathrm{int}}(r) = \frac{g(r)}{\mathcal{K}} - \frac{2}{\pi}\frac{1}{\mathcal{K}}\int_a^r \arcsin\left(\frac{t}{r}\right) g'(t)\,dt. \tag{4.18}$$

In particular, we observe that

$$\frac{\partial u_{z,\mathrm{int}}(r)}{\partial r} = \frac{2}{\pi \mathcal{K} r}\int_a^r \frac{t g'(t)}{(r^2 - t^2)^{1/2}}\,dt. \tag{4.19}$$

Thus, as expected, if g is differentiable with a continuous derivative (which implies the same regularity for F_z), then the gap profile is regular.

Note, however, that, when $g'(t)$ is increasingly peaked and tends to $g'(t) = \Delta g(a)\delta(t - a)$, that is to say when g tends to a function with a discontinuity $\Delta g(a)$ at a, we do tend to the singular JKR flat-punch deformation, $u_{z,fp}$ (Eq. (4.6)), with displacement $g(a)/\mathcal{K}$. Thus, as is now well known, the singular JKR case appears as a limit within a non-singular model.

Up to now, we have given and investigated the general contact equations for a body with arbitrary shape and an arbitrary stress distribution outside the contact zone. We have identified the contributions of two rather different effects: for a given penetration, the part of the stress distribution far away from contact essentially leads to an overall additional attractive force, while no additional deformation close to the contact zone is incurred; the part of the stress distribution close to the contact zone essentially leads to an increase of the contact zone by a spreading-like effect described by the ratio $g(a)/\mathcal{K}$.

5. SELF-CONSISTENT APPROACH

We now tackle the self-consistent part of the approach. Up to now, no hypothesis as to the nature of the stress distribution outside the contact zone was made. Let us now assume that the stress outside

the contact zone is derived from some interaction potential between the surfaces, $V([u])$. An exact self-consistent approach, thus, requires that everywhere outside the contact zone,

$$F_z(r) = -\frac{\partial V}{\partial [u]}([u(r)]); \tag{5.1}$$

Now, as we have just seen, $[u(r)]$ also depends upon $F_z(s)$ in a non-trivial manner. This exact formulation is, thus, difficult to use directly, except for numerical calculations.

Let us rather introduce a weaker (approximate) formulation of the self-consistent approach. The value of the potential for a zero surface separation is some non-zero adhesion energy, w. From this bare definition of the adhesion energy, we obtain the condition:

$$w = \int_a^{+\infty} p(s) \frac{\partial [u]}{\partial s} ds. \tag{5.2}$$

This approximate self-consistency equation will turn out to be quite sufficient to specify the stress distribution to first order outside the contact zone and, thus, describe the adhesive contact.

We first examine the consequences of Eq. (5.2) in the case where the interactions are short-ranged.

5.1. Short Range Interactions – The General JKR Model

If the interaction range is small, the radial extension of the interaction will also be small, g' is peaked around a and, from Eq. (4.19), the dominant term in Eq. (5.2) will be the $\partial u_{z,\text{int}}/\partial s$ term. Thus,

$$w \simeq -\frac{2}{\pi}\frac{1}{K}\int_a^{+\infty} dt\, t g'(t) \int_t^{+\infty} \frac{p(s)ds}{s(s^2 - t^2)^{1/2}} \simeq -\frac{1}{a}\int_a^{+\infty} g'(t)g(t), \tag{5.3}$$

where the s and t factors in the integrals were replaced by a to first order since $p(s)$ decreases rapidly outside the contact zone. As a result, in the case of short-range interactions, the self-consistency equation

boils down to

$$w = \frac{g(a)^2}{\pi \mathcal{K} a}. \tag{5.4}$$

Thus, $g(a)$, which has been shown above to describe completely the adhesive contact in the present case, is determined as a function of w. The generalization of the JKR equations to an arbitrary shape of indenter clearly appears.

5.1.1. Penetration and Force

As a result of Eq. (5.4),

$$g(a) = -(\pi w a \mathcal{K})^{1/2} \tag{5.5}$$

and, taking into account the considerations of Section 4.2.2, the penetration and force are then easily derived from their adhesionless counterparts through Eqs. (4.12) and (4.14):

$$\delta = \delta_0(a) - \left(\frac{\pi w}{\mathcal{K}}\right)^{1/2} a^{1/2} \tag{5.6}$$

$$F = F_0(a) - 4(\pi \mathcal{K} w)^{1/2} a^{3/2}. \tag{5.7}$$

In particular, we clearly observe that the adhesive process is independent of the shape of the indenter.

5.1.2. Fracture Mechanics Approach

Maugis and Barquins have shown that the generalization of the JKR approach can be obtained under the viewpoint of fracture mechanics [10–12]. They have used expansions of the Sneddon expressions to calculate the adhesion-induced stress intensity factor. We now show that the present formulation of the problem also allows a discussion of the same issue directly through the energy release rate. Following these authors, we assume that the interactions are infinitely short-ranged, so that

$$g(a_-) < 0 \tag{5.8}$$

$$g(r) = 0 \quad \text{for } r > a, \tag{5.9}$$

that is to say, there is an attractive stress distribution characterized by $g(a)$ inside the contact zone, but the attractive stress distribution outside the contact zone has been shrunk to zero. Then, from Eq. (3.11), the mechanical energy, $\mathcal{E}$, is

$$\mathcal{E} = \frac{2}{K}\int_0^a ds\, g^2(s). \tag{5.10}$$

5.1.3. Equilibrium

From a fracture mechanics viewpoint, the contact radius, a, is a thermodynamic quantity, and equilibrium is obtained if, for an elementary variation in contact area, dA, the variation in mechanical energy, $d\mathcal{E} = G dA$, is equal to the variation of the interfacial energy, $w\, dA$, or, stated otherwise, if the adhesion energy, here rather acting as a surface tension, is equal to the energy release rate, G.

Now, Eq. (4.9) shows that $g(t)$ is independent of a for $t < a$. Thus, at constant penetration, δ,

$$G = \frac{d\mathcal{E}}{dA} = \frac{1}{2\pi a}\frac{d\mathcal{E}}{da} = \frac{g^2(a)}{\pi K a}, \tag{5.11}$$

from which we again obtain Eq. (5.4).

5.1.4. Stability

Maugis has extensively studied the stability of the equilibrium in various cases. This point is all the more significant as instability means contact rupture: hence, the pull-off force is determined by the stability condition. The system is stable if

$$\frac{d^2\mathcal{E}}{dA^2} > 0 \tag{5.12}$$

Most noteworthy, the stability depends upon the loading conditions, *i.e.*, if in Eq. (5.12) the derivative is taken at constant penetration (fixed grip) or constant force (fixed load). To that purpose, adequate

expressions for G are directly obtained from Eqs. (4.12) and (4.13):

$$g(a) = \mathcal{K}\{\delta - \delta_0(a)\} = \frac{F(a) - F_0(a)}{4a}, \tag{5.13}$$

and

$$G = \frac{\mathcal{K}(\delta - \delta_0(a))^2}{\pi a} = \frac{(F(a) - F_0(a))^2}{16\pi a^3 \mathcal{K}}. \tag{5.14}$$

This last expression for the energy release rate often occurs in Maugis' papers. From these latter expressions, the general stability conditions can be calculated as:

$$\frac{\partial \delta_0}{\partial a} > \frac{-g(a)}{2a\mathcal{K}} \tag{5.15}$$

or

$$\frac{\partial \delta}{\partial a} = 0 \tag{5.16}$$

at fixed grip and

$$\frac{\partial F_0}{\partial a} > -6g(a) \tag{5.17}$$

or

$$\frac{\partial F}{\partial a} = 0 \tag{5.18}$$

at fixed load.

As a result, these expressions show how the shape of the indenter determines the value of the contact radius for which contact break-up occurs and, thus, the pull-off force.

To conclude this subsection, let us consider again Derjaguin's initial paper [1]. Assuming energy balance between the Hertz elastic energy, $2\mathcal{K}a^5/5R^2$, and the interfacial energy, $\pi w a^2$, Derjaguin implicitly assumed that a variation of contact radius leads to a variation of interfacial energy proportional to the full adhesion energy, w, that is to say that the interactions are very short-ranged, and the displacement right outside the contact zone is very steep since it spans the full

decay length of the interaction potential. This concept, central to the JKR theory, is inconsistent with a bare Hertz deformation.

5.2. Intermediate Range Interactions

In the case of intermediate range interactions, the results will depend upon the balance of the long-range and short-range parts of the interaction. Thus, exact results require that the interaction be precisely described. However, we have shown that for reasonably well-behaved interaction potentials, good approximations are obtained when, in addition to the adhesion energy, w, the interaction is simply described by a typical decay length [16]. We will, thus, now describe the approximate analytical models of the JKR-DMT transition one can obtain along this line of thought.

In 1992, Maugis showed, using a constant stress approximation for the attractive interaction (Dugdale model), that an analytical model could be presented for the contact of spheres [9]. The results show that the JKR-to-DMT transition occurs because $g(a)$ decreases to zero while F_{ext} increases to $2\pi wR$ as the range of the interactions increases to infinity (and their amplitude goes to zero, so as to keep w finite).

After Maugis, various approximate models have been developed. One chooses some reasonable form of the stress distribution outside the contact zone: the cases studied thus far were low order polynomials: constant, linear, and quadratic [16]. The distribution, however, is characterized by a radial extension, c, and an amplitude, σ_0. The solution to the contact problem can be completely calculated analytically, as shown above. We, thus, obtain analytical expressions for the force, the penetration, the gap and also for the self-consistency Eq. (5.2) in terms of a, c and σ_0. As a result, for each value of the contact radius, a, and the interaction amplitude, σ_0, the radial extension, c, can be calculated numerically from the self-consistency equation, and the numerical values of the force and penetration determined.

Thus, force curves can be calculated for various values of the interaction amplitude, σ_0. Note that σ_0 and w typically specify the range of the interactions which is of the order w/σ_0. Such approximation schemes have been shown to reproduce closely the results of extensive numerical calculations for definite interaction potentials, at a much lower computational cost [15, 16].

Another kind of approximation has been introduced recently by Johnson and Greenwood [15]. Instead of using a polynomial stress distribution in the attractive interaction zone, they introduced an ellipsoidal distribution, which lends itself more easily to analytical calculations. Actually, we can observe from Eq. (3.9) that this form of interaction stems from a low-order polynomial approximation *on the g function*. In the above mentionned instance [15], one has

$$g(t) \propto (c^2 - t^2) \quad \text{for } a < t < c. \tag{5.19}$$

Thus, one can anticipate a whole class of such approximations, with similar behaviour.

5.3. Long Range Interactions

The long-range interactions seem easy to tackle. In this case, we assume that the interaction zone spreads out far away from the contact zone and, as a result of the finite value of the adhesion energy, the amplitude of the interaction is vanishing. Thus, in the self-consistency equation, Eq. (5.2), the gap is essentially determined by the shape of the indenter, $h(r)$; the additional deformations due to the contact, which typically spread out only as a far as a few times the contact radius, are negligible.

In the discussion, we will keep to integer order indenter shape. The best known case is the case of the paraboloid. There, we have

$$w = \int_a^{+\infty} p(s) \frac{s}{R} ds. \tag{5.20}$$

As a result, as defined in Eq. (3.2) $g(a)$ goes to zero; that is to say, there is no increase of the contact zone. If we compare the adhesion energy, w, and F_{ext}, we directly obtain that

$$w = \frac{1}{2\pi R} F_{\text{ext}}, \tag{5.21}$$

which is the DMT result [2]. Typically, the DMT case is known to apply when a sizeable meniscus of condensed liquid surrounds the contact zone.

If the shape of the indenter is described by a higher-order power law, then $g(a)$ also goes to zero but, in addition, F_{ext} also becomes

small compared with w: only the smaller-ranged part contributes, and this goes to zero.

In contrast, in the case of the cone, we observe that $g(a) \equiv w$ while F_{ext} goes to infinity!

We conclude that, *except in the case of the paraboloid*, it is physically impossible to assume that the interaction zone spreads out far away from the contact zone: in the case of higher-order shapes, the gap slopes up too fast, while, in the case of the cone, the contact zone grows up too fast. In these cases, therefore, we must resort to the intermediate range description when the JKR case does not apply. Note that in the bi-dimensional case (2D), a similar phenomenon has been found when considering the contact of a parabolic indenter: the pull-off force goes to zero when the interaction zone spreads out far from contact, and no "2D-DMT" limit is observed for a parabolic shape [33].

These results do not reduce the relevance of the DMT limit. First of all, the paraboloidal case is *the* significant case, since any axisymmetric non-conformal asperity will adequately be described for all relevant purposes as a paraboloid. Moreover, the existence of this limit is also probably the reason why approximate schemes like those mentioned in Section 5.2 are efficient.

6. INTERACTING SURFACES WITHOUT CONTACT

The assessment of adhesion energies from pull-off forces thus only depends, to first order, upon the range of the relevant interactions. We emphasize the fact that the description of the interacting surfaces before contact, or after contact rupture, should be consistent with the assumptions made for the description of the contact. Thus, if the long-range interactions are measured, their contributions to the total pull-off force may be calculated and the remaining part ascribed to short-range forces, which cannot be measured directly.

Assuming reversible processes throughout, as we did, the non-contact part of the force curve is described by simply specifying the stress distribution

$$F_z(r) = -p(r), \tag{6.1}$$

and the surface deformations computed through Eqs. (3.2) and (3.1). As a result, one obtains a continuous curve taking into account interactions and deformations with and without contact. A good (theoretical) example of such a full force curve can be found in Ref. [8].

Thus, if some assumption is made regarding the interaction between surfaces for the contact part of the curve, one can check whether this assumption is consistent with the measured non-contact part of the curve. Parts of the full curve may be inaccessible, however, due to instability, either plain physical instability, or more often experimental instability, due to the finite stiffness of the measuring system.

In the absence of instability at contact rupture, the contact radius will go to zero, and assuming a regular enough interaction potential, it appears that the force curve will be continuous with a continuous derivative at zero contact radius. Thus, the zero slope in the DMT model at zero contact radius mentioned in the Introduction is due to the fact that the dominant force term, F_{ext}, is a constant equal to $2\pi Rw$. Under consistent assumptions, it will still essentially be constant for some distance after contact rupture, so that the slope after contact rupture is indeed also zero. Thus, if the interaction is such that the slope is not zero after contact rupture, one should conclude that the DMT model is not adequate to describe the contact, and that a more elaborate model like Maugis' or others should be used.

We will now elaborate on the necessary consistency between the treatment of contact and non-contact parts of the force curve using an experimental example. Figure 5 displays the scaled results of the full (backward) force curve measured between silica surfaces in dry air, as obtained with a very rigid surface forces apparatus [34]. The linear non-contact part of the curve allows the long-range interactions to be described as meniscus-induced. Thus, a Maugis model appeared adequate. However, it turned out that it was impossible to fit consistently the contact and non-contact data with a Maugis model because, for the relevant values of the parameters ($\lambda = 0.3$), no force jump appears in the Maugis model. It, thus, became clear that an additional much shorter-ranged force also played a role in the interaction. A proper model taking into account two very different length scales was devised [35], which allowed a good fit of the data, showing that the long-range interaction (the meniscus force, described as in the Maugis model by a constant stress zone, with a λ

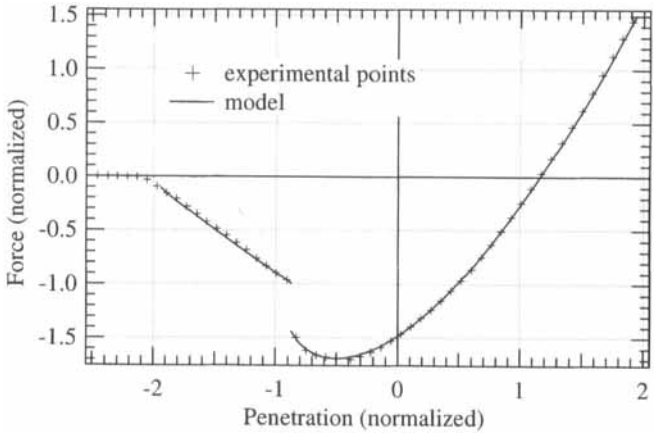

FIGURE 5 Normalized force vs. normalized penetration for a silica/silica contact in dry air. The experimental points are from Ref. [34], the model is described in Section 6 and Ref. [35].

close to 0.3) accounts for about two-thirds and the short-range interaction (described similarly, but with a very large λ arbitrarily taken as 10) for one-third of the total adhesion.

This type of data treatment, therefore, allows some estimate of the very-short-range forces to be obtained through the comparison of long-range forces and pull-off force. We have also tried to use the same approach in the very different context of ultra-high vacuum force measurements between a metal tip and oxide substrates [36].

7. CONCLUSION

We have shown that the Sneddon approach to the elastic response of a flat surface to axisymmetric loadings is convenient to describe the adhesive contact of bodies. It allows general and useful expressions to be derived easily, and highlights the generic features of the various theories. In addition, the useful extension to the case where the surfaces interact but are not in contact is readily obtained.

We have, thus, introduced the generalized JKR model under various aspects. Several approximate models for the intermediate cases have been introduced and classified. The DMT limit has been shown to depend crucially upon the shape of the indenter.

References

[1] Derjaguin, B. V., *Kolloid Z* **69**, 155 (1934).
[2] Derjaguin, B. V., Muller, V. M. and Toporov, Yu. P., *J. Collid Interface Sci.* **53**, 314 (1975).
[3] Johnson, K. L., Kendall, K. and Roberts, A. D., *Proc. Roy. Soc. London A* **324**, 301 (1971).
[4] Tabor, D., *J. Colloids Interface Sci.* **58**, 2 (1977).
[5] Muller, V. M., Yushenko, V. S. and Derjaguin, B. V., *J. Colloids Interface Sci.* **77**, 91 (1980).
[6] Muller, V. M., Yushchenko, V. S. and Derjaguin, B. V., *J. Colloids Interface Sci.* **92**, 92 (1982).
[7] Attard, P. and Parker, J. L., *Phys. Rev. A* **46**, 7959 (1992).
[8] Greenwood, J. A., *Proc. R. Soc. Lond. A* **453**, 1277 (1997).
[9] Maugis, D., *J. Colloids Interface Sci.* **150**, 243 (1992).
[10] Maugis, D. and Barquins, M., *J. Phys. D: Appl. Phys.* **11**, 1989 (1978).
[11] Barquins, M. and Maugis, D., *J. Mech. Theor. Appl.* **1**, 331 (1982).
[12] Maugis, D., *J. Adhesion Sci. Tec.* **1**, 105 (1987).
[13] Johnson, K. L., *Langmuir* **12**, 4510 (1996).
[14] Johnson, K. L. and Greenwood, J. A., *J. Colloid Interface Sci.* **192**, 326 (1997).
[15] Greenwood, J. A. and Johnson, K. L., *J. Phys. D: Appl. Phys.* **31**, 3279 (1998).
[16] Barthel, E., *J. Colloid Interface Sci.* **200**, 7 (1998).
[17] Barthel, E., *Thin Solid Films* **330**, 27 (1998).
[18] Hertz, H., *J. reine und angewandte Mathematik* **92**, 156 (1882).
[19] Hughes, B. D. and White, L. R., *Q. Jl Mech. Appl. Math.* **32**, 445 (1979).
[20] Boussinesq, J., *Application des Potentiels àl'Etude de l'Equilibre et du Mouvement des Solides Elastiques* (Gauthier-Villars, Paris, 1885).
[21] Hamaker, H. C., *Physica* **4**, 1058 (1937).
[22] Sneddon, I. N., *Fourier Transform* (McGraw-Hill, New York, 1951).
[23] Muki, R., "Progress in solid mechanics", In: Sneddon, I. N. and Hill, R. Eds., *Progress in Solid Mechanics*, I (North Holland, Amsterdam, 1960), Chap. VIII, p. 399.
[24] Spence, D. A., *Proc. Roy. Soc. A* **305**, 55 (1968).
[25] Gladwell, G. M. L., *Contact Problems in Linear Elasticity* (Sijthoff and Noordhoff, Alphen aan den Rijn, 1980).
[26] Johnson, K. L., *Contact Mechanics* (Cambridge University Press, Cambridge, 1985).
[27] Fogden, A. and White, L. R., *J. Colloid Interface Sci.* **138**, 414 (1990).
[28] Hills, D. A. J., Nowell, D. and Sackfield, A., *Mechanics of Elastic Contacts* (Butterworth-Heinemann, 1993).
[29] Basire, C. and Fretigny, C., *C. R. Acad. Sci. Paris* **326**, 323 (1998).
[30] Landau, L. D. and Lifsitz, E. M., *Theory of Elasticity*, 2nd edn. (Pergamon Press, Oxford, 1970).
[31] Sneddon, I. N., *Int. J. Eng. Sci.* **3**, 47 (1965).
[32] Lowengrub, M. and Sneddon, I. N., *Int. J. Eng. Sci.* **3**, 451 (1965).
[33] Baney, J. M. and Hui, C. Y., *Adhes. Sci. Techol.* **11**, 393 (1997).
[34] Barthel, E., Lin, X. Y. and Loubet, J. L., *J. Colloid Interface Sci.* **177**, 401 (1996).
[35] Barthel, E., *Colloids and Surfaces A* **149**, 99 (1999).
[36] Sounilhac, S., Barthel, E. and Creuzet, F., *J. Appl. Phys.* **85**, 222 (1999).

APPENDIX A

We describe the linear elastic response of a flat solid submitted to an axisymmetric normal stress distribution, F_z. Let us start from the

mechanical equilibrium condition

$$\mathrm{div}(\bar{\bar{\sigma}}) + \bar{F} = 0, \tag{A1}$$

and the linear elasticity relation

$$\bar{\bar{\sigma}} = \frac{\nu E}{(1-2\nu)(1+\nu)}\mathrm{Tr}(\bar{\bar{\varepsilon}})\bar{\bar{\delta}} + \frac{E}{(1+\nu)}\bar{\bar{\varepsilon}}, \tag{A2}$$

where $\bar{\bar{\sigma}}$ is the stress tensor, $\bar{\bar{\varepsilon}}$ the strain tensor, $\bar{F}$ the external stress distribution, $\bar{\bar{\delta}}$ the unit tensor and E and ν the Young's modulus and Poisson's ratio. We will write down an equation for the displacement field, u, knowing that the strain tensor is the symmetric part of the gradient of the displacement field.

We now take the axisymmetric nature of the problem into account by resorting to the form of Fourier transform which arises in such conditions, *i.e.*, the Hankel transform. Indeed, in the angular integration of the Fourier transform, one comes across the quantity

$$\int_0^{2\pi} \exp(ikr\cos(\theta))d\theta, \tag{A3}$$

which directly leads to the use of Bessel functions like

$$J_0(r) = \frac{1}{\pi}\int_0^{\pi} \cos(r\cos(\theta))d\theta \tag{A4}$$

and Hankel transforms. In addition, we take into account the tensorial nature of the fields we are looking for by noting that the normal components, u_z, and, F_z, of the displacement and force fields transform as scalars under a rotation around the z axis, while the tangential components u_r and F_r transform as vectors. As a result, we will selectively use the Hankel transforms of order 0 and 1 as follows:

$$\tilde{u}_{z,0}(k,z) = \int_0^{+\infty} drr\,J_0(kr)u_z(r,z), \tag{A5}$$

$$\tilde{F}_{z,0}(k,z) = \int_0^{+\infty} drr\,J_0(kr)F_z(r,z), \tag{A6}$$

$$\tilde{u}_{r,1}(k,z) = \int_0^{+\infty} drr\,J_1(kr)u_r(r,z), \tag{A7}$$

$$\tilde{F}_{r,1}(k,z) = \int_0^{+\infty} dr r J_1(kr) F_r(r,z), \tag{A8}$$

where J_1 is the first-order Bessel function

$$J_1(r) = \frac{1}{\pi}\int_0^{\pi} \sin(r\cos(\theta))\cos(\theta)d\theta. \tag{A9}$$

From the expressions for the divergence and gradient in cylindrical coordinates, and the properties of Hankel transforms, one obtains the following equilibrium conditions on the displacement field

$$\left(-\alpha^2 k^2 + \frac{\partial^2}{\partial z^2}\right)\tilde{u}_{r,1}(k,z) - \beta k \frac{\partial}{\partial z}\tilde{u}_{z,0}(k,z) = -\frac{2(1+\nu)}{E}\tilde{F}_{r,1}(k,z), \tag{A10}$$

$$\beta k \frac{\partial}{\partial z}\tilde{u}_{r,1}(k,z) + \left(\alpha^2 \frac{\partial^2}{\partial z^2} - k^2\right)\tilde{u}_{z,0}(k,z) = -\frac{2(1+\nu)}{E}\tilde{F}_{z,0}(k,z), \tag{A11}$$

with

$$\alpha^2 = \frac{2(1-\nu)}{1-2\nu} \tag{A12}$$

and

$$\beta = \frac{1}{1-2\nu}. \tag{A13}$$

If we now assume that the tangential component, F_r, of the force field is zero, Eq. (A10) becomes

$$\mathcal{O}_1 \tilde{u}_{r,1}(k,z) - \mathcal{O}_2 \tilde{u}_{z,0}(k,z) = 0, \tag{A14}$$

where the operators are defined as

$$\mathcal{O}_1 = -\alpha^2 k^2 + \frac{\partial^2}{\partial z^2}, \tag{A15}$$

$$\mathcal{O}_2 = \beta k \frac{\partial}{\partial z}. \tag{A16}$$

Now $\mathcal{O}_1$ and $\mathcal{O}_2$ commute, so that one can introduce a potential function, $G(k,z)$, such that, from Eq. (A14),

$$\tilde{u}_{z,0}(k,z) = \mathcal{O}_1 G(k,z), \tag{A17}$$

$$\tilde{u}_{r,1}(k,z) = \mathcal{O}_2 G(k,z). \tag{A18}$$

Then Eq. (A14) is automatically fulfilled and since

$$\beta = \alpha^2 - 1, \tag{A19}$$

Equation (A11) becomes

$$\left(\frac{\partial^2}{\partial z^2} - k^2\right)^2 G(k,z) = -\frac{(1+\nu)(1-2\nu)}{(1-\nu)E}\tilde{F}_{z,0}(k,z), \tag{A20}$$

which provides a solution for a solid submitted to an axisymmetric distribution of normal stress.

1. Elastic Surface Loaded Axisymmetrically

Let us now examine the response of a flat elastic surface submitted to a normal stress distribution. We now introduce the boundary conditions relevant for the surface. The plane of the surface will be chosen as $z=0$. All fields and, thus, the potential $G(k,z)$, vanish above the surface ($z > 0$). We assume that the external forces are described by the *surface* distribution, $\tilde{F}_{z,0}(k)\delta(z)$. We are now essentially looking for $G_{\text{sing.}}(k,z)$, the singular part of $G(k,z)$, which will give rise to the δ function on the right-hand side of Eq. (A20). Given the fact that $G(k,z)$ is zero in the upper half-space, a cosine transform (on the negative part of the z axis) is in order. Introducing the cosine transform of $G_{\text{sing.}}(k,z)$ (denoted $\tilde{G}_{\text{sing.}}(k,\xi)$), the solution to Eq. (A20) is obtained as

$$\tilde{G}_{\text{sing.}}(k,\xi) = -\frac{(1+\nu)(1-2\nu)}{(1-\nu)E}\tilde{F}_{z,0}(k)\frac{1}{2\pi}\frac{1}{(\xi^2+k^2)^2}, \tag{A21}$$

from which, by inverse cosine transform, one gets

$$G_{\text{sing.}}(k,z) = -\frac{(1+\nu)(1-2\nu)}{2(1-\nu)E}\tilde{F}_{z,0}(k)\frac{1}{k^2}\left(\frac{1}{k} - z\right)\exp(kz) \tag{A22}$$

for $z < 0$. By definition, $G_{\text{sing.}}(k,z)=0$ for $z \geq 0$. This expression provides a solution of the mechanical equilibrium equation, which expresses the balance of forces, when a surface is subjected to a surface distribution, $F_z(r)$, of normal forces. It is not, however, a solution for a *free* surface, for the surface shear, in this solution, is not zero. Therefore, we now build the zero-surface shear solution.

2. Frictionless Elastic Surface Loaded Axisymmetrically

The general solution to Eq. (A20) is made up of the singular part we have just calculated plus a regular term of the form $(A+Bz)\exp(-kz)+(C+Dz)\exp(+kz)$, where A, B, C and D depend only upon k. Keeping only the term $G_{\text{reg.}}(k,z)=(C+Dz)\exp(+kz)$ which vanishes when z goes to $-\infty$, the general potential is now

$$G(k,z) = G_{\text{sing.}}(k,z) + G_{\text{reg.}}(k,z). \tag{A23}$$

The boundary conditions on the free surface are, using the obvious notation:

$$\sigma_{zz,\text{reg.}}(k,z)|_{z=0} = 0 \tag{A24}$$

$$\sigma_{rz,\text{reg.}}(k,z)|_{z=0} + \sigma_{rz,\text{sing.}}(k,z)|_{z=0} = 0. \tag{A25}$$

Applying the Hankel transform of order 0 to Eq. (A24) and the Hankel transform of order 1 to Eq. (A25), again in agreement with their tensorial nature, one gets

$$\nu\beta k\tilde{u}_{r,1,\text{reg.}}(k,z) + \frac{\alpha^2}{2}\frac{\partial}{\partial z}\tilde{u}_{z,0,\text{reg.}}(k,z) = 0 \tag{A26}$$

$$\frac{\partial}{\partial z}\tilde{u}_{r,1}(k,z) - k\tilde{u}_{z,0}(k,z) = 0. \tag{A27}$$

From the definitions of $G(k,z)$, $\tilde{u}_{r,1}(k,z)$ and $\tilde{u}_{z,0}(k,z)$ (Eqs. (A23), (A17) and (A18)) one obtains a system of two linear equations in C and D, from which the final solution for a frictionless

axisymmetrically loaded elastic surface is obtained as:

$$\tilde{u}_{r,1}(k,z) = \left(\frac{1+\nu}{E}\left(\frac{1-2\nu}{k}+z\right)\tilde{F}_{z,0}(k)\right)\exp(kz) \tag{A28}$$

$$\tilde{u}_{z,0}(k,z) = \left(\frac{2(1+\nu)}{E}\left(\frac{1-\nu}{k}-\frac{z}{2}\right)\tilde{F}_{z,0}(k)\right)\exp(kz). \tag{A29}$$

For contact problems, the important general result is that, at the surface ($z=0$),

$$\tilde{u}_{z,0}(k) = \frac{2(1-\nu^2)}{E}\frac{\tilde{F}_{z,0}(k)}{k}, \tag{A30}$$

where $\tilde{u}_{z,0}(k)$ [resp. $\tilde{F}_{z,0}(k)$] denotes $\tilde{u}_{z,0}(k,z=0)$ [resp. $\tilde{F}_{z,0}(k,z=0)$].

This expression is clearly the equivalent of Landau's $1/r$ Green's function in real space [30]. Since $k\tilde{u}_{z,0}(k)$ is essentially the transform of the gradient of $u_z(r)$, this relation simply states that the normal compliance of the surface is $\mathcal{K}^{-1}$.

APPENDIX B: USEFUL FORMS OF THE GENERAL RESULT AND ITS RELEVANCE TO MIXED BOUNDARY CONDITIONS

As a result of Eq. (A30) and using the inverse Hankel transform (the form of which is identical to the direct transform), one can express the surface displacement as:

$$u_z(r) = \frac{2(1-\nu^2)}{E}\int_0^{+\infty}\tilde{F}_{z,0}(k)J_0(kr)dk. \tag{B1}$$

Now, with the change of variable $t = r\cos\theta$ in Eq. (A4), one obtains the following expression for the Bessel function:

$$J_0(kr) = \frac{2}{\pi}\int_0^r \frac{\cos(kt)dt}{(r^2-t^2)^{1/2}}, \tag{B2}$$

that is to say, the Bessel function of order 0 is also the cosine transform of the function

$$\frac{\Theta(r-t)}{(r^2-t^2)^{1/2}}, \tag{B3}$$

where Θ is the usual Heaviside step function.

Indeed, let us now introduce the cosine transform of the quantity $\tilde{F}_{z,0}(k)$, which is itself the Hankel transform of the axisymmetric surface stress distribution:

$$g(t) = \int_0^{+\infty} \tilde{F}_{z,0}(k)\cos(kt), \tag{B4}$$

one readily gets Eqs. (3.1) and (3.2), by using, for instance, Parseval's relation:

$$u_z(r) = \frac{4}{\pi}\frac{(1-\nu^2)}{E}\int_0^r \frac{g(t)}{(r^2-t^2)^{1/2}}dt,$$

and similarly,

$$g(t) = \int_t^{+\infty} \frac{sF_z(s)}{(s^2-t^2)^{1/2}}ds.$$

This trick in the inverse Hankel transform allows one to dispense altogether with dual integral equations [22] and Erdelyi-Kober operators [27]. Now the adequation of this form of solution to mixed boundary conditions becomes obvious since $u_z(r)$ depends *only* on the values of $g(t)$ smaller than r, while $F_z(s)$ depends *only* on the values of $g(t)$ larger than s.

In addition, Eqs. (3.1) and (3.2) can both be inverted through the use of inverse Hankel and Fourier transforms, leading to the inverse relations (3.6), (3.7), (3.8) and (3.9).

Let us introduce two additional useful properties of this representation. The total force exerted on the surface F can be easily expressed as (Eq. (3.10))

$$F = 2\pi\int_0^{+\infty} drrF_z(r) = 2\pi\tilde{F}_{z,0}(k=0) = 2\pi\frac{2}{\pi}\int_0^{+\infty} dsg(s),$$

where the second equality stems from the Hankel transform and the last from cosine transform.

Similarly, the total mechanical energy, $\mathcal{E}$, can be calculated using Parseval's relation for the Hankel and the cosine transform (Eq. (3.11))

$$\mathcal{E} = \pi \int_0^{+\infty} drrF_z(r)u_z(r) = \pi \int_0^{+\infty} dkk\tilde{F}_{z,0}(k)\tilde{u}_{z,0}(k)$$
$$= \frac{\pi}{\mathcal{K}} \int_0^{+\infty} dk\tilde{F}_{z,0}(k)^2 = \frac{2}{\mathcal{K}} \int_0^{+\infty} dsg^2(s),$$

where the second equality comes from the Parseval's relation for the Hankel's transform, the third from the equilibrium relation Eq. (A30), and the fourth from Parseval's relation for cosine transform.